Prognostic value of Urokinase-type Plasminogen Activator Receptor (uPAR)-PET/CT in Head and Neck Squamous Cell Carcinomas and Comparison with ^{18}F-FDG-PET/CT: A single-center prospective study

Running title: Prognostic value of uPAR-PET in HNSCC

Louise M. Risør[1], Malene M. Clausen[2], Zaza Ujmajuridze[3], Mohammed Farhadi[3], Kim F. Andersen,[1], Annika Loft[1], Jeppe Friborg[2], Andreas Kjaer[1,*]

[1]Department of Clinical Physiology, Nuclear Medicine and PET & Cluster for Molecular Imaging, Copenhagen University Hospital – Rigshospitalet & Department of Biomedical Sciences, University of Copenhagen, Denmark

[2]Department of Clinical Oncology, Copenhagen University Hospital, Rigshospitalet, Copenhagen, Denmark

[3]Department of Clinical Oncology, Næstved Hospital, Denmark

*Corresponding author: Prof. Andreas Kjaer, MD, PhD, DMSc, E-mail: akjaer@sund.ku.dk

Address: Department of Clinical Physiology, Nuclear Medicine & PET. Rigshospitalet, Blegdamsvej 9, DK 2100 Copenhagen, Denmark

First author: PhD student Louise Madeleine Risør, MD, E-mail: louise.madeleine.risoer@regionh.dk

Address: Department of Clinical Physiology, Nuclear Medicine & PET. Rigshospitalet, Blegdamsvej 9, DK 2100 Copenhagen, Denmark

Word count: 4855

ABSTRACT

Purpose

The aim of this phase II trial (NCT02965001) was to evaluate the prognostic value of urokinase-type plasminogen activator receptor (uPAR)-PET/CT with the novel ligand 68Ga-NOTA-AE105 in head and neck cancer and compare it to 18F-fluorodeoxyglucose (18F-FDG).

Materials and methods

Patients with head and neck squamous cell carcinoma (HNSCC) referred to curatively intended radiotherapy were eligible and prospectively included in this phase II study. A 68Ga-uPAR- and 18F-FDG-PET/CT were performed before initiation of curatively intended radiotherapy and maximum standardized uptake values (SUVmax) of the primary tumor was measured on both PET/CTs by two independent readers. Relapse-free survival (RFS) and overall survival (OS) were calculated and optimal cut-off values were established for 68Ga-uPAR- and 18F-FDG-PET independently and compared using log rank and Kaplan-Meier statistics, and univariate and multivariate analysis in Cox proportional hazards model.

Results

A total of 57 patients were included and followed for a median of 33.8 months (range 2.30-47.2). The median SUVmax of the primary tumors were 2.98 (range 1.94-5.24) for 68Ga-uPAR and 15.7 (range 4.24-45.5) for 18F-FDG. The optimal cut-off points for 68Ga-NOTA-AE105 SUVmax in the primary tumor was 2.63 for RFS and 2.66 for OS. A high uptake of 68Ga-NOTA-AE105 (SUVmax above cut-off) was significantly associated with poor RFS and OS (log-rank p=0.012 and p=0.022). 68Ga-NOTA-AE105-uptake in the primary tumor was significantly associated with poor RFS in univariate analysis (HR=8.53 (95% confidence interval (CI) 1.12-64.7), p=0.038) and borderline associated with OS (HR=7.44 (95% CI 0.98-56.4), p=0.052).

For 18F-FDG-PET, the optimal cut-off points were 22.7 for RFS and 22.9 for OS. 18F-FDG SUVmax above cut-off was significantly associated with reduced RFS (log-rank p=0.012) and OS (log-rank p=0.000). 18F-FDG-uptake was significantly associated with reduced RFS and OS in univariate analysis (HR=3.27; 95% CI 1.237-8.66), p=0.017) and (HR=7.10; 95% CI 2.60-19.4), p<0.001). In a multivariate analysis including 68Ga-uPAR SUVmax, 18F-FDG SUVmax, Tumor, Node and Metastasis (TNM) stage and p16 status, only 68Ga-uPAR SUVmax remained significant (HR 8.51 (95%CI 1.08-66.9), p=0.042) for RFS. For OS, only TNM stage and 18F-FDG remained significant.

Conclusion

The current phase II clinical trial showed promising results for the use of 68Ga-uPAR-PET SUVmax in the primary tumor to predict RFS in HNSCC patients referred to curatively intended radiotherapy when compared to 18F-FDG-PET, TNM stage and p16 status. 68Ga-uPAR-PET could potentially become valuable for identification of patients suited for de-escalation of treatment and risk stratified follow-up schemes.

Key words: Urokinase-type Plasminogen Activator Receptor (uPAR), 68Ga-NOTA-AE105, PET/CT, Head and Neck Cancer, prognostication, risk stratification, molecular imaging.

INTRODUCTION

Traditionally, head and neck squamous cell carcinoma (HNSCC) is caused by alcohol and tobacco, but in recent years a rising incidence of oropharyngeal cancers (OPSCC) has been associated with human papillomavirus (HPV)(*1*). HPV-positive tumors currently accounts for 63 % of the OPSCC in Western Europe and have a significantly favorable prognosis (*2,3*). HPV-positive and HPV-negative OPSCC represent distinct molecular and clinical entities and new staging guidelines reduce the stage allocation of HPV-positive tumors based on p16 immunohistochemistry as a surrogate marker of HPV driven carcinogenesis (*3,4*). However, recent clinical trials investigating de-escalating treatment regimens in low-risk HPV-positive OPSCC resulted in inferior survival of the de-escalating arms (*5-8*). To date no reliable method of identifying candidates for de-escalating treatment exists and HPV-positive and negative OPSCC are treated alike (*3,9*).

Tumor, Node and Metastasis (TNM) stage and HPV are the most important prognostic factors in HNSCC, but besides HPV no prognostic biomarkers are available in clinical practice. Regarding the prognostic value of 18F-FDG, inconsistent results have been published(*9-11*).

The urokinase-type Plasminogen Activator Receptor (uPAR) promotes cancer cell invasion by degrading the extracellular matrix and facilitates several carcinogenic processes e.g. proliferation and migration (*12-14*). High uPAR expression has been reported in many cancer types, including HNSCC and has been associated with aggressive disease, distant metastasis and poor survival (*14*). uPAR is located on the cell surface and has limited expression in the surrounding tissue (*13*). Phase I studies using 68Ga- and 64Cu-labeled AE105-radioligands for uPAR-PET in patients with different cancer types have supported the theory of uPAR being target-specific and encouraged research exploring the potential of uPAR-PET as a non-invasive theragnostic agent (*15-17*).

The aim of the current phase II study was to investigate the prognostic value of 68Ga-NOTA-AE105 uPAR-PET in HNSCC patients and to compare it with 18F-FDG-PET.

MATERIAL AND METHODS

Patient population

Inclusion criteria were patients with a diagnosis of biopsy-verified cancer of the pharynx, larynx or oral cavity, referred to curatively intended radiotherapy, who understood the given information, was able to give informed consent and age above 18 years.

Exclusion criteria were pregnancy, lactation/breast feeding, age above 85 years, obesity (bodyweight above 140 kg), small cancers of the larynx (1A,1B), allergy to 68Ga-NOTA-AE105, metastasis on FDG-PET/CT, other previously known cancers and claustrophobia. Eligible patients were included after giving informed consent. Diagnosis of HNSCC and p16 status was verified histologically prior to inclusion. Information on smoking, alcohol, clinical examination, treatment plan, laboratory and histological results, medical history and follow-up examinations were collected from patient records. Disease stage was coded according to Union for International Cancer Control (UICC) 8th edition.

The study protocol was approved by the Danish Health and Medicine Authority (EudraCT no. 2016-002082-65) and the Ethical Committee of the Capital Region of Denmark (protocol no. H-16039798). Signature of written informed consent was obtained from all patients. The study was registered in ClinicalTrials.gov (NCT02965001) and performed in accordance with the recommendation for Good Clinical Practice (GCP) including independent monitoring by the GCP unit of the Capital Region of Denmark.

68Ga-uPAR-PET/CT acquisition

According to national guidelines on treatment of HNSCC, radiotherapy is to be initiated within 11 days of the treatment decision and 18F-FDG-PET/CT and 68Ga-uPAR-PET/CT were performed

within this period, both as a part of the prospective study. In order to minimize the risk of osteonecrosis following radiotherapy, patients underwent a dental examination and in the case of teeth extraction, initiation of radiotherapy was postponed until two weeks after the procedure. In this case, 18F-FDG-PET/CT and 68Ga-uPAR-PET/CT was scheduled before or at least 4 days after the procedure.

All patients were injected intravenously with approximately 200 MBq (median 191, range 158-209 MBq) of 68Ga-NOTA-AE105 followed by sequential whole-body PET/CT scanning 20 min post-injection. Whole-body 68Ga-NOTA-AE105 PET and diagnostic CT with contrast (skull base to proximal thigh) was performed simultaneously using an integrated whole-body PET/CT (Siemens Biograph mCT 64 slice, Siemens, Erlangen, Germany). Synthesis of the ligand was performed as previously described (15).

Patients were immobilized in the supine position on a flat scanner couch with arms placed in standard anatomical position and no fixating facial mask was applied. The CT scan was performed with 120kV, 170 MAS, pitch 0.8. The PET data was reconstructed with an iterative reconstruction method using time of flight, point spread function and attenuation corrections with 2 iterations, 21 subsets and a 2 mm Gaussian filter.

Image Analysis

Image data from the 68Ga-uPAR-PET/CT and 18F-FDG-PET/CT was analyzed by two certified specialists in nuclear medicine. The readers were blinded to the volumes of interest (VOIs), results of the other reader and patient information. Volumes of interest were visually contoured on the 68Ga-uPAR-PET/CT corresponding to the localization of the primary tumor on the 18F-FDG-PET/CT. Uptake of the 68Ga-uPAR ligand and 18F-FDG in the volumes of interest were parameterized as SUVmax on the 68Ga-uPAR-PET/CT and 18F-FDG-PET/CT and documented for both tracers before obtaining information of recurrences and survival.

If a patient had two synchronous primary HNSCCs, the tumor with the highest SUVmax was included in the statistical analysis. The mean value of the SUVmax obtained by the two independent readers was included in the statistical analysis.

Treatment and Follow-up

All patients received intensity-modulated radiotherapy (IMRT) with or without concomitant chemotherapy according to national guidelines (*18*). All patients received a prescribed dose of 66 to 68 Gy in 33 to 34 fractions, 6 fractions per week and one patient received proton radiation. Patients with advanced disease, if assessed fit, received concomitant cisplatin administered weekly (40 mg/m2); all patients with normal liver and renal function tests and no neurologic symptoms received a hypoxic radiosensitizer (nimorazole) daily (1200 mg/m2). According to national guidelines all HNSCC patients attended a 5-year follow-up program. All patients attended the follow-up program throughout the study period and concurrent diseases, visits to other departments and deceased individuals were followed through the Danish personal identity number.

Statistical Analysis

A sample size of 104 patients was calculated as needed for the study based on ability to detect a HR of 2.5 with a power of 70% (beta: 30%) and a level of significance (alpha) of 5% and a follow up of 2 years. However, due to the slowdown in performing clinical studies caused by the COVID-19 pandemic the study was delayed, but with a longer follow-up the needed number of events was reached.

Clinical endpoints were relapse-free survival (RFS) defined as time from diagnosis to any relapse of the disease at the locoregional (TN site) and/or distant metastasis (M site) with deaths from other causes recorded as censoring and disease-free survival (DFS), which is defined as RFS, but includes death of any reason as an event. Loco-regional control (LRC) was defined as time from

diagnosis to relapse at the locoregional site with deaths and distant metastasis recorded as censoring. Overall survival (OS) was defined as time from diagnosis to death of any cause. Follow-up time was calculated from the time of referral to radiotherapy until first relapse, death or until end of follow-up January 1st, 2021.

Determination of the optimal cut-off in discrimination between favorable and poor prognosis was performed with Cut-off finder, an R-package developed by Budczies et al.(*19*). Associations between biomarker expression beneath or above cut-off and survival outcomes were visualized in Kaplan-Meier plots using the log-rank test to assess significance of differences. Hazard ratios were estimated in univariable and multivariable Cox proportional hazards model in which the PET parameters were included as binarized parameters according to the defined cut-offs for RFS and OS.

The number of events included in the survival analysis were: 17 events in RFS and 16 events in OS analysis. Based on the number of events, four predictors were the maximal number of explanatory variables that could reasonably be included in the final multivariable Cox model. In addition to the aim of testing the prognostic value of 68Ga-uPAR SUVmax and compare it to 18F-FDG SUVmax, TNM stage and p16 status (p16-positive OPSCC versus all other tumors) were also included in the multivariable analysis, since they are the most important non-imaging prognostic factors in HNSCC (9). Model performance was estimated using Harrell's Concordance Index (C-index).

Interrater reliability of SUV-measurement was estimated using intraclass correlation coefficient (ICC).

A p-value of < 0.05 was considered statistically significant. Statistical analyses were performed using IBM SPSS Statistics v. 22 (IBM Corp. Armonk, NY) and R (http://www.Rproject.org).

RESULTS

Patients

A total of fifty-seven patients recently diagnosed with HNSCC in the pharynx, larynx or oral cavity and referred to curatively intended radiotherapy at Rigshospitalet and Næstved Hospital, Denmark, were consecutively included in the current prospective phase II study from December 2017 – November 2019, Figure 1. None of the patients experienced reactions or adverse events related to the administration of 68Ga-NOTA-AE105. One patient terminated the 68Ga-NOTA-AE105-(uPAR)-PET/CT scan due to claustrophobia and two patients were diagnosed with unknown primary tumor (UPT) of the head and neck after a lymph node biopsy and were excluded from the statistical analysis. Patient characteristics are shown in Table 1. More than half the patients (59.2 %) presented with early stage disease (Stage 1-2) and 38.9 % had no primary regional nodal disease. Moreover, 61.1 % were located in the oropharynx of which 78.7 % were p16 positive. Median follow-up was 33.8 months (range 2.30-47.2).

Clinical Follow-up

Histological verification of loco-regional recurrences was obtained in 15/16 patients serving as reference for the study outcome. One patient did not have a histological verification of the loco-regional recurrence but had active tumor at the primary site on 18F-FDG-PET/CT and histologically verified lung metastases. Biological material from biopsy or surgery was available from all (3) patients with suspected distant metastasis. Consequently, we did not experience missing data regarding recurrences and the two patients with unknown primary tumors (UPT) were excluded due to missing data from the primary tumor. No patients were lost to follow-up and clinicopathological information was collected before inclusion.

Seventeen patients (31.5 %) were diagnosed with a recurrence, 7 (13.0 %) at the primary site (T site), 5 (9.3 %) at the primary site and lymph nodes (TN site), 2 (3.7 %) in the lymph nodes (N site), and 3 (5.6 %) were diagnosed with distant metastases in the lungs (M site). Two of the patients were classified as residual tumor at the 2 months follow-up. Ten of the 17 recurrences (58.8 %) were p16 negative, while seven (41.2 %) were p16 positive tumors. 30 % (3/10) of the loco-regional recurrences were p16 positive and all patients (3/3) with distant metastases were confirmed p16 positive. All 17 patients who experienced a relapse completed all fractions of the primary radiotherapy.

During follow-up 16 patients (29.6 %) died; 8 (14.8 %) due to HNSCC and 8 (14.8 %) due to non-HNSCC causes; 1 (1.9 %) died due to sepsis 1 month after treatment, 1 died due to exacerbation of Chronic Obstructive Pulmonary Disease (COPD), 1 due to lung embolism (diagnosed and successfully operated for a recurrence prior to his death), 1 discontinued his routine treatment of HIV and died due to infection, 1 died of rectal cancer, 2 of lung cancer, and 1 died of unknown causes, but without any sign of recurrence at the follow-up 2 months prior to his death. None of the non-cancer deaths had signs of recurrence at the previous follow-up. The patient who died of sepsis 1 month after treatment before the first routine follow-up was included in the statistical analyses as not having an event. Imaging performed in the acute phase in the case of sepsis and exacerbation of COPD had no sign of recurrence. 4 out of 6 patients who died due to HNSCC were p16 negative (66.7 %), while 2 (33.3 %) were p16 positive.

68Ga-uPAR- and 18F-FDG-uptake

The median SUVmax of the primary tumors were 2.98 (range 1.94-5.24) for 68Ga-uPAR-uptake and 15.7 (range 4.24-45.5) for 18F-FDG-uptake, Figure 2. The median time interval between the 68Ga-uPAR- and 18F-FDG-PET/CT was 2.4 days (range 1-4).

Cut-off Points and Kaplan-Meier Curves

The optimal cut-off points were determined as the point with the most significant split in the Kaplan-Meier plot (log-rank test) and the corresponding hazard ratios (HRs) including 95% confidence intervals were calculated (*19*). For 68Ga-uPAR the cut-points were 2.63 for RFS and 2.66 for OS, separating the patients in a group of 41 (75.6%) above cut-off and 13 (24.1%) below cut-off in RFS analysis and a group of 40 (74.1%) above and 14 (25.9%) below cut-off in OS analysis. For 18F-FDG-PET, the optimized cut-points were 22.7 for RFS and 22.9 for OS, separating a group of 42 (77.8%) patients below and 12 (22.2%) patients above cut-off in RFS analysis, and a group of 43 (79.6%) patients below and 11 (20.4%) patients above cut-off in OS analysis.

Kaplan-Meier curves combined with log-rank analysis for differences showed a significant association between poor RFS (log-rank p=0.012) and OS (log-rank p=0.02) and high 68Ga-uPAR SUVmax above cut-off. Similarly, 18F-FDG SUVmax above cut-off was significantly associated with reduced RFS (p=0.012) and OS (p <0.001), Figure 3.

Survival Analysis

Univariate and multivariate analysis using Cox proportional hazards model are summarized in Table 2. In univariate analysis high uptake of 68Ga-uPAR (above cut-off) in the primary tumor was significantly associated with reduced RFS (HR=8.53 (95% confidence interval (CI) 1.12-64.7), p=0.038) and borderline significant associated with OS (HR=7.44 (95% CI 0.981-56.44), p=0.052). High uptake of 18F-FDG was significantly associated with reduced RFS and OS (HR=3.27 (95% CI 1.237-8.66), p=0.017) and (HR=7.10(95% CI 2.60-19.4), p<0.001). High TNM stage (S3-4) was significantly associated with both RFS (HR=3.46 (95% CI 1.216-9.88), p=0.020) and OS (HR=6.72 (95% CI 2.12-21.4), p=0.001). In multivariable analysis, including 68Ga-uPAR SUVmax, 18F-FDG SUVmax, TNM stage and p16, only 68Ga-uPAR SUVmax remained significantly associated with RFS (HR 8.50 (95%CI 1.11-65.3), p=0.040), but not with respect to OS (HR = 4.58 (95% CI 0.583-36.0),

p=0.148). For OS, high 18F-FDG SUVmax (HR=4.986 (95% CI 1.658-14.990), p=0.004) and TNM

stage (HR=3.856 (95% CI 1.114-13.343), p=0.033) remained significantly associated. In DFS analysis,

the results reflected the fact that DFS is a combination of RFS and OS events, Supplemental Table 1.

We did not have statistical power to conclude on LRC due to too few events, but the results showed

the same trend as RFS.

In post-hoc analysis, inclusion of 68Ga-uPAR SUVmax in the multivariate cox-model improved

the predictive performance in RFS analysis (C-index: 0.74 to 0.78) and for 18F-FDG (C-index: 0.76 to

0.78). In OS analysis inclusion of 68Ga-uPAR SUVmax improved the predictive performance (C-index:

0.81 to 0.84) and for 18F-FDG (C-index: 0.80 to 0.84). The C-index for a model only including TNM

stage and p16 was 0.70 for RFS and 0.77 for OS.

68Ga-uPAR and 18F-FDG Concordance

In post-hoc analysis, combining 68Ga-uPAR-PET and 18F-FDG into groups of 1) both scans

low, 2) one scan high/one scan low and 3) both scans high according to the established cut-offs,

demonstrated a concordance rate near 40 % for RFS and OS and a discordance rate near 60% for

RFS and OS . The distribution of the groups is shown in table 3 and Kaplan-Meier curves in figure 4.

Overall, there was a significant difference between the groups in RFS and OS analysis (log-rank

p=0.001). For RFS and OS, the concordant both high groups had a significantly poorer RFS compared

to the concordant both low groups (p<0.0001). The group with discordant one low/one high uptake

had an intermediate prognosis with a significantly more favorable prognosis compared to the both high

group for both RFS and OS (p= 0.006 and p<0.0001), but inferior to the both low group, although not

reaching significance (p=0.110 and p=0.069).

Interrater Reliability

Interrater reliability in measurement of tumor SUVmax was good with an ICC of 0.835 (95% CI 0.713-0.905).

DISCUSSION

The main finding of the current prospective phase II study was the ability of 68Ga-uPAR-PET/CT with 68Ga-NOTA-AE105 to predict RFS in HNSCC patients referred to curatively intended radiotherapy. In univariate analysis 18F-FDG-SUVmax also predicted RFS, however, in a multivariate analysis including 68Ga-uPAR-SUVmax, 18F-FDG-SUVmax, TNM stage and p16 immunohistochemistry, only 68Ga-uPAR-SUVmax remained significant.

Accordingly, we demonstrated that a primary tumor 68Ga-uPAR-PET SUVmax cut-off could be established for identification of high- and low-risk groups in HNSCC patients referred to curatively intended radiotherapy. The PET parameter SUVmax is simple to obtain and the most frequently reported and most reproducible PET uptake metric in the literature ([20]).

The large proportion 8/16 (50%) of the non-HNC related deaths found in our study may explain why 68Ga-uPAR-PET was not able to predict OS. The poor general health status of many HNSCC patients is known to result in a high number of non-HNSCC deaths due to competing risks following tobacco and alcohol consumption ([21]). However, our study was not powered to evaluate 68Ga-uPAR-PET in predicting HNSCC-related deaths.

Since uPAR expression takes part in the tumor invasion and metastatic process ([12,14]), it is not surprising that high levels of uPAR-PET is related to relapse. Previous phase I clinical trials of 68Ga-uPAR-PET ([16,17,22]) as well as an array of preclinical studies ([13,23-26]) have demonstrated that our 68Ga-uPAR-PET indeed visualizes uPAR expression.

18F-FDG-PET SUVmax is the most common and well-characterized PET-uptake metric and a proposed prognostic marker in various cancers. Therefore, in our study we predefined 18F-FDG-PET SUVmax for comparison. For HNSCC, several studies have concluded that 18F-FDG-PET SUVmax does hold prognostic information, but results are inconsistent. Most of the studies are retrospective cohort studies and a concern has been that 18F-FDG is simply a surrogate marker of known clinical risk factors, especially tumor size (*10,11*). However, our results support the evidence of SUVmax being a significant predictor of patient outcome for both 68Ga-uPAR and 18F-FDG in univariate analysis.

18F-FDG is not tumor-specific and various image interpretation pitfalls exist due to physiological uptake and the complex anatomy of the head and neck (*27*). We found that 18F-FDG-PET SUVmax could predict OS but not RFS in the multivariate model. 68Ga-uPAR-PET remained significant regarding RFS in the multivariate model, but not 18F-FDG-PET, which demonstrates that the prognostic information obtained with 68Ga-uPAR is different from 18F-FDG-PET. The two tracers may be used for different purposes and complement each other in providing detailed non-invasive whole-tumor characterization (*28-30*). 68Ga-uPAR and 18F-FDG concordance could supply additional information to a future risk stratification of low (both low), intermediate (one low/one high) and high-risk patients (both high) for personalized treatment and follow-up strategies.

The more recent 18F-FDG-PET-uptake metrics metabolic tumor volume (MTV) and total lesion glycolysis (TLG) have shown promising prognostic results and inclusion of such parameters in future and larger phase studies could be of interest (*31*). Nonetheless, these parameters have several limitations and no consensus regarding volume segmentation and threshold have been established (*31*). For 68Ga-uPAR-PET prognostication we believe that SUVmax is the relevant metric for characterization of the most aggressive phenotype within the tumor and as a predictor of prognosis rather than a measure of volumes.

The current study represents a first proof-of-concept in a moderately sized study population. Larger future prospective (Phase III) studies are needed to establish the exact cut-off values that may also depend on the exact composition of the population. Nevertheless, with the current SUVmax cut-off point at 2.63, we identified the 25 % of patients with low risk of recurrence. Due to the considerable toxicity associated with chemoradiotherapy, initiatives to de-escalate the treatment for selected patients are being explored and 68Ga-uPAR may assist with a reliable identification of such low-risk patients (*7*).

Moreover, there is considerable variation in surveillance strategies following head-neck cancer treatment (*32*). Routine imaging is not standardized, and often patients request fewer follow-up visits (*33*). If results are validated, 68Ga-uPAR-PET may contribute to the development of risk stratified follow-up schedules.

In the past decades research in optimizing treatment for HNSCC patients has focused on the geometric precision of radiotherapy, but a shift towards biological precision has begun. The prognostic strength of 68Ga-uPAR-PET is the quantitative read out from tumor lesions and not a visual delineation, as some tumors may have low and almost no uptake. Accordingly, 68Ga-uPAR-PET will not replace 18F-FDG-PET as a diagnostic tool. In addition, 68Ga-uPAR-PET/CT may become an important companion diagnostics for selection of patients eligible for uPAR-targeted optical guided surgery using a uPAR-targeted optical probe or uPAR-targeted radionuclide therapy as well as for planning of external radiation therapy with customization of uPAR-targeted dose delivery of IMRT in patients with high tumor uptake (*23,34-37*).

CONCLUSION

The current phase II clinical trial evaluating the prognostic impact of 68Ga-uPAR-PET/CT using 68Ga-NOTA-AE105 showed that 68Ga-uPAR-PET SUVmax can predict RFS in HNSCC patients referred to curatively intended radiotherapy. In a multivariate analysis including 68Ga-uPAR

SUVmax, 18F-FDG SUVmax, TNM stage and p16 status only 68Ga-uPAR SUVmax remained significant for RFS. For OS, TNM stage and 18F-FDG SUVmax were significant.

Abbreviations

68Ga: Gallium-68

AE105: Ac-Asp-Cha-Phe-(D)Ser-(D)Arg-Tyr-Leu-Trp-Ser-CONH$_2$

NOTA : *2,2',2"-(1,4,7-triazacyclononane-1,4,7-triyl)triacetic acid*

Disclosures

Disclaimer

AK is an inventor on a patent of the composition of matter of uPAR PET (WO 2014086364) and co-founder of Curasight, which has licensed the uPAR PET technology. No other potential conflicts of interest relevant to this article exist.

KEY POINTS

Research question: What is the prognostic value of the novel ligand 68Ga-NOTA-AE105 for uPAR-PET/CT in head and neck cancer (HNSCC).

Pertinent findings: High primary tumor uptake of the uPAR-PET-tracer was associated with poor relapse-free survival in HNSCC patients, whereas FDG-PET was associated with poor OS.

Implications for patient care: uPAR-PET/CT offers a potential tool for clinicians to select low-risk HNSCC patients for de-escalated treatment regimens to avoid unnecessary toxicity and for a risk stratified follow-up schedule.

REFERENCES

1.   Chaturvedi AK, Engels EA, Pfeiffer RM, et al. Human papillomavirus and rising oropharyngeal cancer incidence in the United States. *J Clin Oncol.* 2011;29:4294-4301.

2.   Mehanna H, Franklin N, Compton N, et al. Geographic variation in human papillomavirus-related oropharyngeal cancer: Data from 4 multinational randomized trials. *Head Neck.* 2016;38 Suppl 1:E1863-1869.

3.   Albers AE, Qian X, Kaufmann AM, Coordes A. Meta analysis: HPV and p16 pattern determines survival in patients with HNSCC and identifies potential new biologic subtype. *Sci Rep.* 2017;7:16715.

4.   O'Sullivan B, Huang SH, Su J, et al. Development and validation of a staging system for HPV-related oropharyngeal cancer by the International Collaboration on Oropharyngeal cancer Network for Staging (ICON-S): a multicentre cohort study. *Lancet Oncol.* 2016;17:440-451.

5.   Jakobsen KK, Gronhoj C, Jensen DH, et al. Increasing incidence and survival of head and neck cancers in Denmark: a nation-wide study from 1980 to 2014. *Acta Oncol.* 2018;57:1143-1151.

6.   Craig SG, Anderson LA, Schache AG, et al. Recommendations for determining HPV status in patients with oropharyngeal cancers under TNM8 guidelines: a two-tier approach. *Br J Cancer.* 2019;120:827-833.

7.   Gillison ML, Trotti AM, Harris J, et al. Radiotherapy plus cetuximab or cisplatin in human papillomavirus-positive oropharyngeal cancer (NRG Oncology RTOG 1016): a randomised, multicentre, non-inferiority trial. *Lancet.* 2019;393:40-50.

8.   Mehanna H, Robinson M, Hartley A, et al. Radiotherapy plus cisplatin or cetuximab in low-risk human papillomavirus-positive oropharyngeal cancer (De-ESCALaTE HPV): an open-label randomised controlled phase 3 trial. *Lancet.* 2019;393:51-60.

9.   Burd EM. Human papillomavirus laboratory testing: the changing paradigm. *Clin Microbiol Rev.* 2016;29:291-319.

10.   Clausen MM, Vogelius IR, Kjaer A, Bentzen SM. Multiple testing, cut-point optimization, and signs of publication bias in prognostic FDG-PET imaging studies of head and neck and lung cancer: A review and meta-analysis. *Diagnostics (Basel).* 2020;10:1030.

11.   Rasmussen JH, Vogelius IR, Fischer BM, et al. Prognostic value of 18F-fludeoxyglucose uptake in 287 patients with head and neck squamous cell carcinoma. *Head Neck.* 2015;37:1274-1281.

12. Dass K, Ahmad A, Azmi AS, Sarkar SH, Sarkar FH. Evolving role of uPA/uPAR system in human cancers. *Cancer Treat Rev.* 2008;34:122-136.

13. Persson M, Kjaer A. Urokinase-type plasminogen activator receptor (uPAR) as a promising new imaging target: potential clinical applications. *Clin Physiol Funct Imaging.* 2013;33:329-337.

14. Mekkawy AH, Pourgholami MH, Morris DL. Involvement of urokinase-type plasminogen activator system in cancer: an overview. *Med Res Rev.* 2014;34:918-956.

15. Skovgaard D, Persson M, Brandt-Larsen M, et al. Safety, dosimetry, and tumor detection ability of (68)Ga-NOTA-AE105: First-in-human study of a novel radioligand for uPAR PET imaging. *J Nucl Med.* 2017;58:379-386.

16. Skovgaard D, Persson M, Kjaer A. Urokinase plasminogen activator receptor-PET with (68)Ga-NOTA-AE105: First clinical experience with a novel PET ligand. *PET Clin.* 2017;12:311-319.

17. Persson M, Skovgaard D, Brandt-Larsen M, et al. First-in-human uPAR PET: Imaging of cancer aggressiveness. *Theranostics.* 2015;5:1303-1316.

18. Guidelines Dahanca. www.dahanca.dk/guidelines (In Danish), Accessed on October 1st 2020.

19. Budczies J, Klauschen F, Sinn BV, et al. Cutoff Finder: a comprehensive and straightforward web application enabling rapid biomarker cutoff optimization. *PLoS One.* 2012;7.

20. Wahl RL, Jacene H, Kasamon Y, Lodge MA. From RECIST to PERCIST: Evolving considerations for PET response criteria in solid tumors. *J Nucl Med.* 2009;50 Suppl 1:122S-150S.

21. Gillison ML, Zhang Q, Jordan R, et al. Tobacco smoking and increased risk of death and progression for patients with p16-positive and p16-negative oropharyngeal cancer. *J Clin Oncol.* 2012;30:2102-2111.

22. Skovgaard D, Persson M, Kjaer A. Imaging of prostate cancer using rokinase-Type Plasminogen Activator Receptor PET. *PET Clin.* 2017;12:243-255.

23. Persson M, Madsen J, Ostergaard S, et al. Quantitative PET of human urokinase-type plasminogen activator receptor with 64Cu-DOTA-AE105: implications for visualizing cancer invasion. *J Nucl Med.* 2012;53:138-145.

24. Persson M, Hosseini M, Madsen J, et al. Improved PET imaging of uPAR expression using new (64)Cu-labeled cross-bridged peptide ligands: comparative in vitro and in vivo studies. *Theranostics.* 2013;3:618-632.

25. Persson M, Liu H, Madsen J, Cheng Z, Kjaer A. First (18)F-labeled ligand for PET imaging of uPAR: in vivo studies in human prostate cancer xenografts. *Nucl Med Biol.* 2013;40:618-624.

26. Persson M, El Ali HH, Binderup T, et al. Dosimetry of 64Cu-DOTA-AE105, a PET tracer for uPAR imaging. *Nucl Med Biol.* 2014;41:290-295.

27. Purohit BS, Ailianou A, Dulguerov N, Becker CD, Ratib O, Becker M. FDG-PET/CT pitfalls in oncological head and neck imaging. *Insights Imaging.* 2014;5:585-602.

28. Marcu LG, Reid P, Bezak E. The promise of novel biomarkers for head and neck cancer from an imaging perspective. *Int J Mol Sci.* 2018;19:2511.

29. Song IH, Noh Y, Kwon J, et al. Immuno-PET imaging based radioimmunotherapy in head and neck squamous cell carcinoma model. *Oncotarget.* 2017;8:92090-92105.

30. Christensen A, Kiss K, Lelkaitis G, et al. Urokinase-type plasminogen activator receptor (uPAR), tissue factor (TF) and epidermal growth factor receptor (EGFR): tumor expression patterns and prognostic value in oral cancer. *BMC Cancer.* 2017;17:572.

31. Rijo-Cedeno J, Mucientes J, Seijas Marcos S, et al. Adding value to tumor staging in head and neck cancer: The role of metabolic parameters as prognostic factors. *Head Neck.* 2021;43:2477-2487.

32. Wong WL. PET-CT for staging and detection of recurrence of head and neck cancer. *Semin Nucl Med.* 2021;51:13-25.

33. Trinidade A, Kothari P, Andreou Z, Hewitt RJ, O'Flynn P. Follow-up in head and neck cancer: patients' perspective. *Int J Health Care Qual Assur.* 2012;25:145-149.

34. Christensen A, Juhl K, Persson M, et al. uPAR-targeted optical near-infrared (NIR) fluorescence imaging and PET for image-guided surgery in head and neck cancer: proof-of-concept in orthotopic xenograft model. *Oncotarget.* 2017;8:15407-15419.

35. Ling CC, Humm J, Larson S, et al. Towards multidimensional radiotherapy (MD-CRT): biological imaging and biological conformality. *Int J Radiat Oncol Biol Phys.* 2000;47:551-560.

36. Atallah I, Milet C, Henry M, et al. Near-infrared fluorescence imaging-guided surgery improves recurrence-free survival rate in novel orthotopic animal model of head and neck squamous cell carcinoma. *Head Neck.* 2016;38 Suppl 1:E246-255.

37. Persson M, Madsen J, Ostergaard S, Ploug M, Kjaer A. 68Ga-labeling and in vivo evaluation of a uPAR binding DOTA- and NODAGA-conjugated peptide for PET imaging of invasive cancers. *Nucl Med Biol.* 2012;39:560-569.

Figure 1: Consort flow diagram of inclusion process

Invited to participate (n = 337)

Enrollment

•Declined to participate (n = 92)
•Referred to palliative radiotherapy (n = 45)
•Not included due to overlap in standard-of-care preparatory examinations and uPAR time slots (n = 143)

Included (n = 57)

Excluded (n = 3)
•Discontinued uPAR-PET/CT scan due to claustrophobia (n = 1)
•Diagnosed with UPT (n = 2)

Analyzed (n = 54)

Follow-Up & Analysis

Recurrences (n = 17)   Death (n = 16)
Locoregional (n = 14)   HNC death (n = 8)
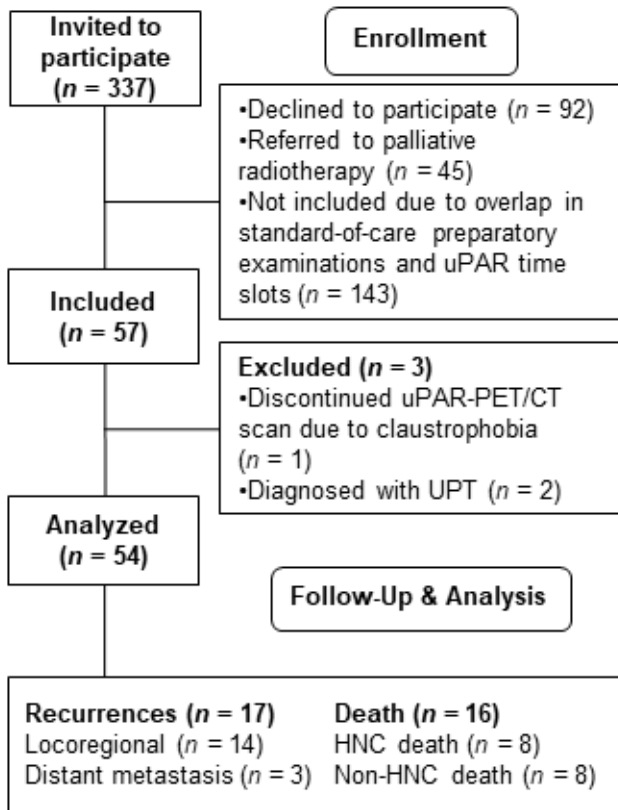Distant metastasis (n = 3)   Non-HNC death (n = 8)

Figure 2: Delineated tumor volumes of interest in uPAR-PET/CT with 68Ga-NOTA-AE105 and 18F-FDG-PET/CT in two cases of discordant high 68Ga-uPAR/low 18F-FDG (A) and low 68Ga-uPAR/high 18F-FDG (B). Both cases present with stage 3 oropharyngeal cancer (T3N0M0). High and low refers to above or below the established cut-offs.
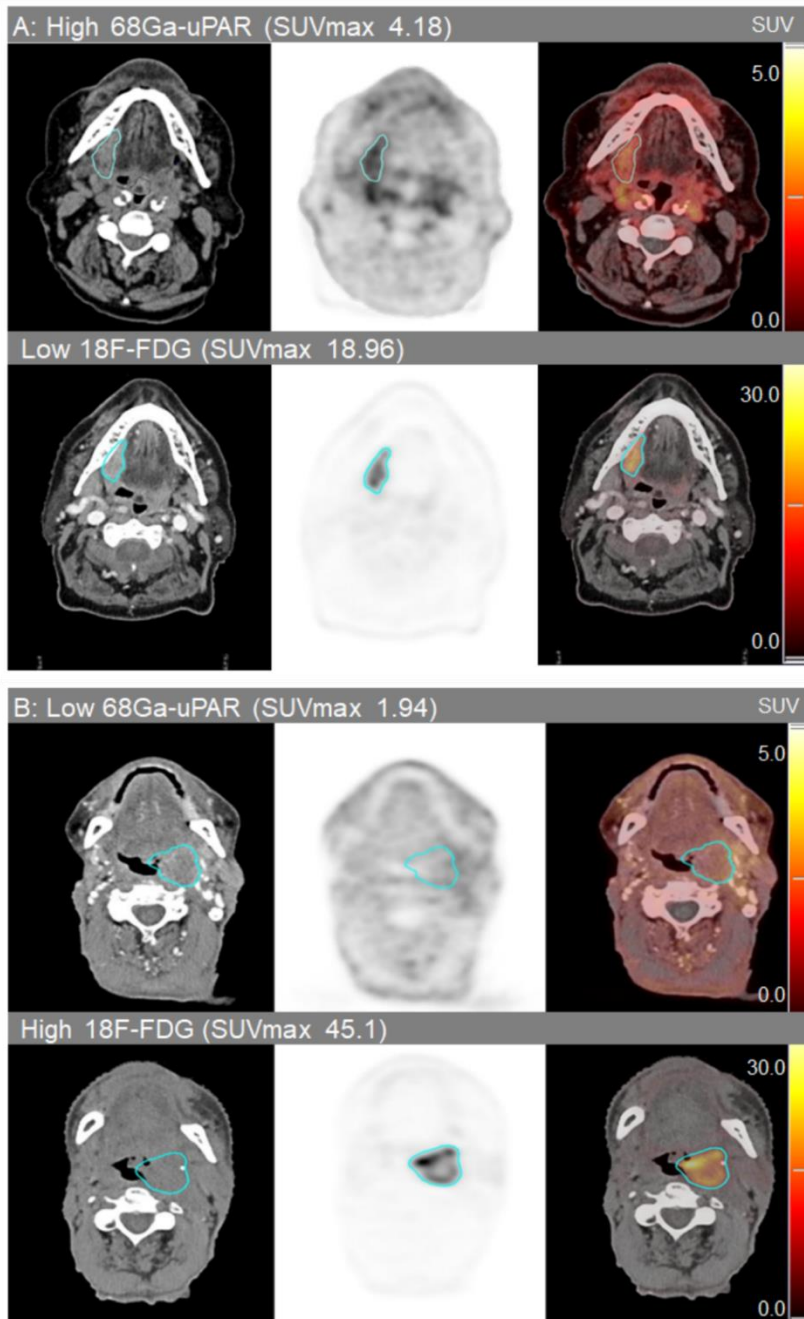
Figure 3: Kaplan–Meier plots of RFS for 68Ga-uPAR (A), OS for 68Ga-uPAR (B), RFS for 18F-FDG (C) and OS for 18F-FDG (D) stratified by the corresponding 68Ga-uPAR- and 18F-FDG-SUVmax cut-offs.
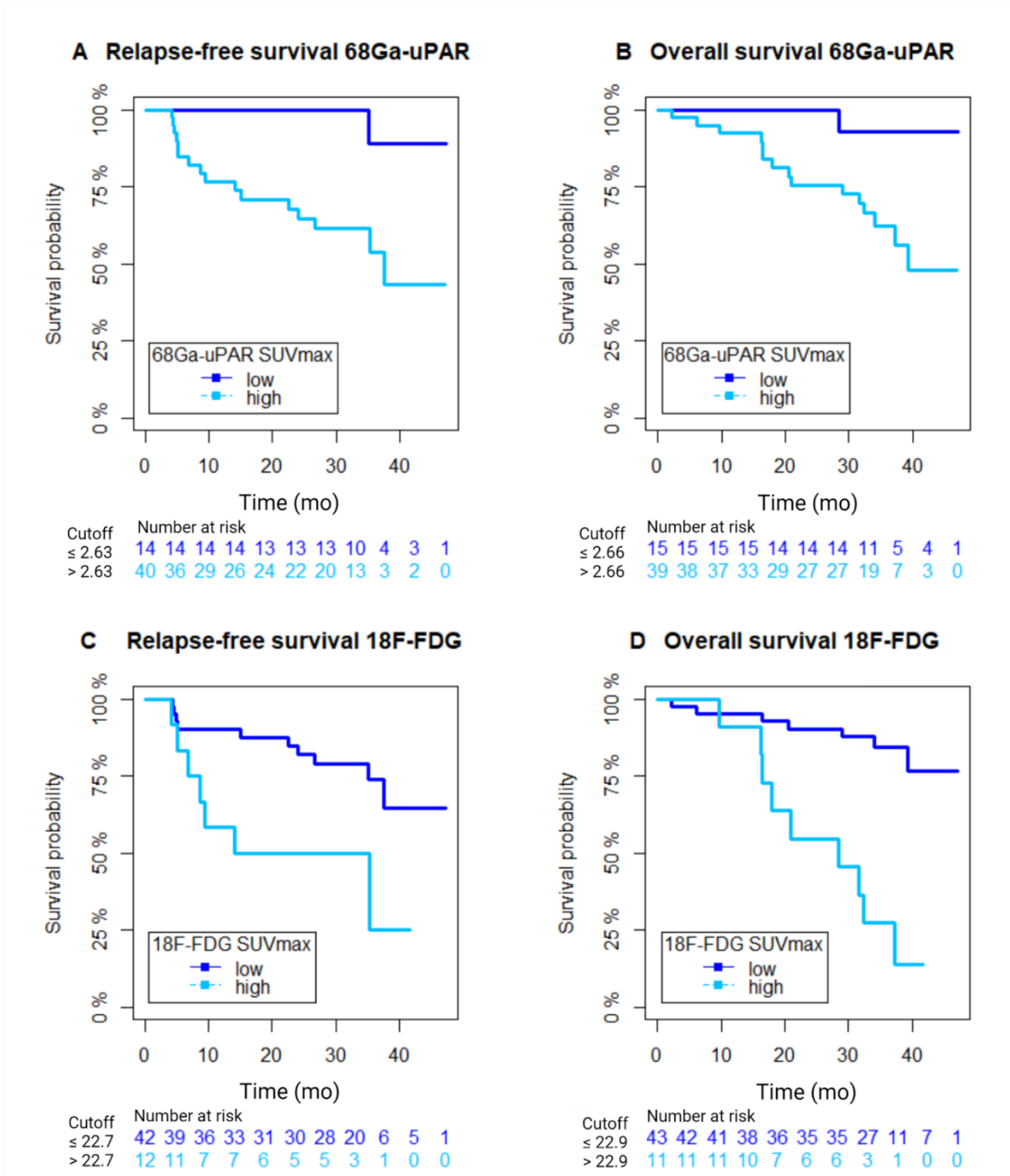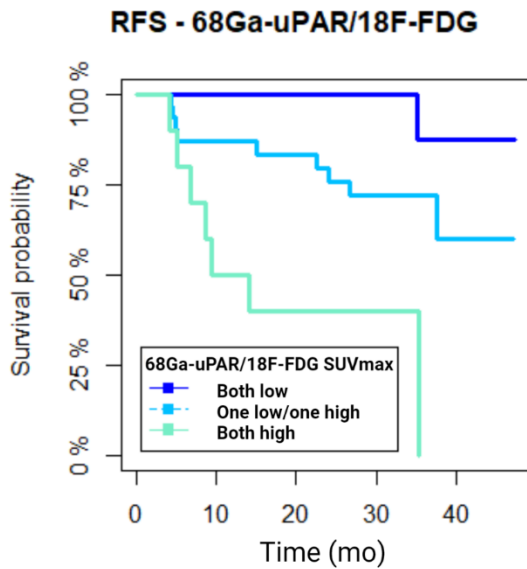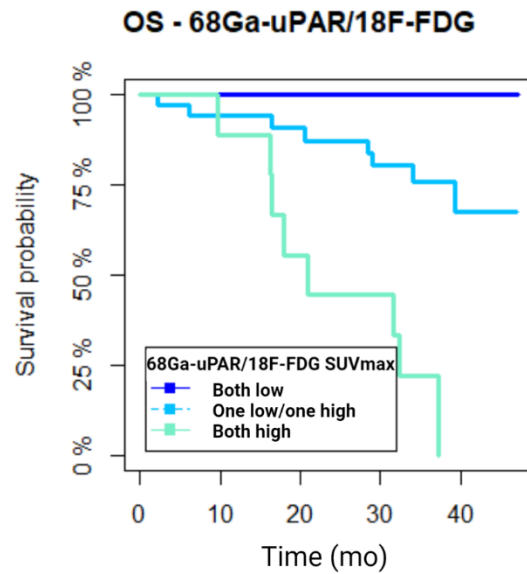
Figure 4: Kaplan-Meier plots of Relapse-free survival (RFS) (A) and Overall survival (OS) (B) for the concordant and discordant groups; 68Ga-uPAR and 18F-FDG both low (dark blue); one low/one high (turquoise); and both high (green).

Table 1: Patient Characteristics. PS Performance status; EBV Epstein Barr Virus; T tumor; N node. *Stage according to UICC 8th edition.

No. of patients			Total	%
			54	100
Sex	Male		45	83.3
	Female		9	16.7
Age	Mean		67.1	
	Range		48-84	
PS	0		51	94.4
	1		3	5.6
Smoking	Never smokers		8	14.8
	Former smokers		24	44.4
	Current smokers		22	40.7
	Pack years (mean)		36.7	(Range 0-150)
Primary site	Oral Cavity		3	5.6
	Pharynx	Rhinopharynx	2	3.7
		Oropharynx	33	61.1
		Hypopharynx	8	14.8
	Larynx		8	14.8
P16 (oropharynx)	p16 positive		26	(78.7)
	p16 negative		7	(21.2)
EBV positive			1	1.9
Stage*	I		12	22.2
	II		20	37.0
	III		9	16.7
	IV		13	24.1
T classification	T1		4	7.4
	T2		26	48.1
	T3		13	24.1
	T4		11	20.4
N classification	N0		21	38.9
	N1		14	25.9
	N2		19	35.2
Chemotherapy	No cisplatin		25	46.3
	Cisplatin		29	53.7
Nimorazole	No		5	9.3
	Yes		49	90.7

Table 2: 3 Cox proportional hazards model for RFS and OS in relation to clinicopathological variables and 68Ga-uPAR- and 18F-FDG-uptake. *Age was included as a continuous covariate. T tumor; N node; M metastasis.
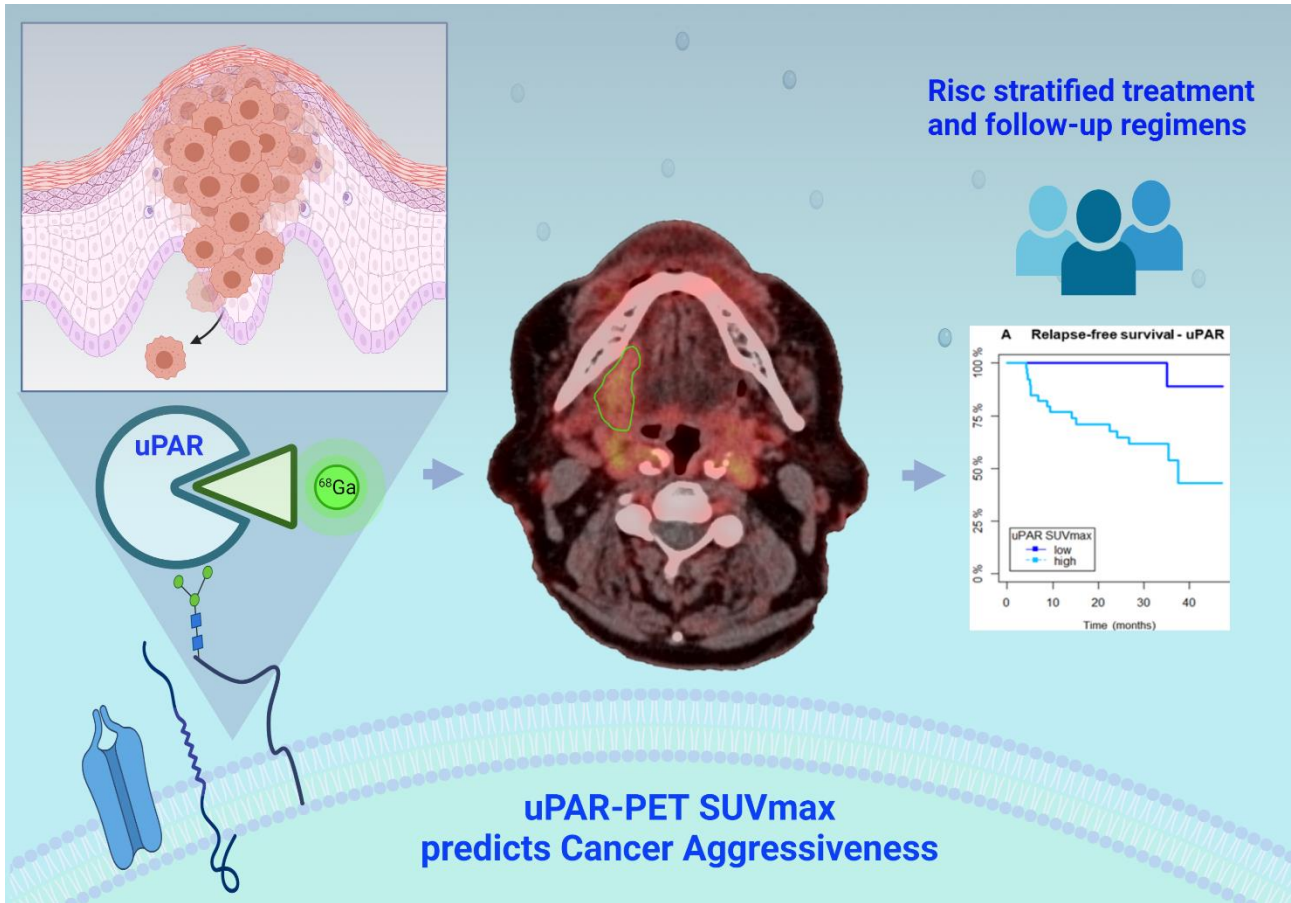
Variables:		n	Relapse-free survival (RFS)						Overall survival (OS)					
			Univariate analysis			Multivariate analysis			Univariate analysis			Multivariate analysis		
			HR	95% CI	p-value	HR	95% CI	p-value	HR	95% CI	p-value	HR	95% CI	p-value
Gender	Women	9												
	Men	45	3.666	0.486-27.657	0.208				3.109	0.410-23.578	0.273			
Age*														
			0.993	0.943-1.046	0.802				1.035	0.984-1.090	0.184			
Smoking	<30 pack years	29												
	>30 pack years	25	1.129	0.433-2.947	0.804				3.072	1.060-8.906	**0.039**			
TNM stage	S1-2	32												
	S3-4	22	3.458	1.211-9.875	**0.020**	2.702	0.827-8.832	0.100	6.724	2.117-21.355	**0.001**	4.309	1.239-14.984	**0.022**
p16	Positive	26												
	Negative	28	2.361	0.864-6.456	0.094	1.006	0.331-3.064	0.991	4.615	1.314-16.212	**0.017**	1.712	0.438-6.691	0.440
68Ga-uPAR	<cutoff	13												
	>cutoff	41	8.530	1.124-64.743	**0.038**	8.511	1.082-66.949	**0.042**	7.439	0.981-56.415	0.052	4.584	0.583-36.044	0.148
18F-FDG	<cutoff	42												
	>cutoff	12	3.266	1.231-8.662	**0.017**	2.240	0.724-6.933	0.162	7.098	2.602-19.360	**0.000**	4.285	1.362-13.479	**0.013**

Table 3: Distribution of patients according to cut-off values for 68Ga-uPAR-PET and 18F-FDG-PET SUVmax for RFS (A) and OS (B).

A) RFS Concordance	uPAR low	uPAR high	Total
FDG low	12 (22.2 %)	30 (55.6 %)	42 (77.8 %)
FDG high	2 (3.7 %)	10 (18.5 %)	12 (22.2 %)
Total	14 (25.9 %)	40 (74.1 %)	54 (100 %)

B) OS Concordance	uPAR low	uPAR high	Total
FDG low	12 (22.2 %)	31 (57.4 %)	43 (79.6 %)
FDG high	2 (3.7 %)	9 (16.7 %)	12 (20.4 %)
Total	14 (25.9 %)	40 (74.1 %)	54 (100 %)

Graphical Abstract

Supplemental Table 1: Cox proportional hazards model for Disease-free survival (DFS) in relation to clinicopathological variables and uPAR- and 18F-FDG-uptake. T tumor; N node; M metastasis

Disease-free survival (DFS)								
			Univariate analysis			Multivariate analysis		
Variables:		n	p-value	HR	95% CI	p-value	HR	95% CI
Gender	Women	9						
	Men	45	0.246	2.360	0.553-10.073			
Smoking	<30 pack years	29						
	>30 pack years	25	0.264	1.604	0.700-3.679			
TNM stage	S1-2	32						
	S3-4	22	0.000	5.088	2.048-12.640	0.005	4.209	1.547-11.449
p16	positive	26						
	negative	28	0.023	2.829	1.158-6.912	0.673	1.235	0.464-3.287
68Ga-uPAR	<cutoff	13						
	>cutoff	41	0.019	5.678	1.323-24.370	0.029	5.224	1.186-23.010
18F-FDG	<cutoff	42						
	>cutoff	12	0.009	3.078	1.321-7.176	0.293	1.665	0.644-4.302